JOURNAL OF TISSUE ENGINEERING AND REGENERATIVE MEDICINE
J Tissue Eng Regen Med 2016; **10**: E177–E187.
Published online 20 June 2013 in Wiley Online Library (wileyonlinelibrary.com) **DOI:** 10.1002/term.1782

RESEARCH ARTICLE

Comparative study of the osteogenic ability of four different ceramic constructs in an ectopic large animal model

Véronique Viateau[1,3], Mathieu Manassero[1,3], Luc Sensébé[2], Alain Langonné[2], David Marchat[4], Delphine Logeart-Avramoglou[1], Hervé Petite[1] and Morad Bensidhoum[1]*

[1]*Laboratory of Bioengineering and Biomechanics for Bone Articulation (B2OA – UMR CNRS 7052), University of Paris 7, PRES Paris Cité, Paris, France*
[2]*Etablissement Français du Sang Centre-atlantique, UMR5273 CNRS/UPS/EFS, Tours, France*
[3]*Ecole Nationale Vétérinaire d'Alfort, Maisons Alfort, France*
[4]*CIS, Ecole Nationale Supérieure des Mines de Saint-Etienne, Saint-Etienne, France*

Abstract

Tissue-engineered constructs combining bone marrow mesenchymal stem cells with biodegradable osteoconductive scaffolds are very promising for repairing large segmental bone defects. Synchronizing and controlling the balance between scaffold-material resorption and new bone tissue formation are crucial aspects for the success of bone tissue engineering. The purpose of the present study was to determine, and compare, the osteogenic potential of ceramic scaffolds with different resorbability. Four clinically relevant granular biomaterial scaffolds (specifically, Porites coral, Acropora coral, beta-tricalcium phosphate and banked bone) with or without autologous bone marrow stromal cells were implanted in the ectopic, subcutaneous-pouch sheep model. Scaffold material resorption and new bone formation were assessed eight weeks after implantation. New bone formation was only detected when the biomaterial constructs tested contained MSCs. New bone formation was higher in the Porites coral and Acropora coral than in either the beta-tricalcium phosphate or the banked bone constructs; furthermore, there was a direct correlation between scaffold resorption and bone formation. The results of the present study provide evidence that, among the biomaterials tested, coral scaffolds containing MSCs promoted the best new bone formation in the present study. Copyright © 2013 John Wiley & Sons, Ltd.

Received 20 March 2012; Revised 24 January 2013; Accepted 24 April 2013

Keywords **bone tissue engineering; bone formation; mesenchymal stem cells; ceramic scaffolds; osteogenesis; scaffold resorption; osteoconduction**

1. Introduction

Endogenous tissue regeneration mechanisms are not sufficient to repair large segmental long-bone defects. Free cortical graft transfer, cancellous bone autograft, and distraction osteogenesis have proven successful in clinical practice (de Boer and Wood, 1989; May *et al*., 1989; Han *et al*., 1992). However, some of these procedures require large quantities of autologous bone graft and, sometimes, repeated surgery in order to achieve bone union. Although autologous bone graft remains the gold standard for bone repair, the pertinent surgical technique is limited by the donor site morbidity, which increases with the amount of harvested bone. In addition, repeated surgical procedures carry the risk of infection and chronic pain, which are common complications.

The possibility of isolating and expanding *in vitro* autologous mesenchymal stem cells (MSCs), starting from a small sample of bone marrow and driving them towards differentiation into the osteogenic phenotype (Friedenstein *et al*., 1966, 1968) has motivated exploration and development of procedures combining bone marrow MSCs with osteoconductive scaffolds; the result

*Correspondence to: M. Bensidhoum, Laboratoire de Bioingénierie et Biomécanique Ostéo-Articulaires (B2OA), UMR CNRS 7052, Université Paris Diderot, 10 Avenue de Verdun, 75010 Paris, France. E-mail: morad.bensidhoum@paris7.jussieu.fr

is known as 'bioengineered bone constructs' (Bianco and Robey, 2001; Cancedda *et al.*, 2003; Caplan, 2005; Logeart-Avramoglou *et al.*, 2005). The proof of concept for such a strategy using MSCs loaded within massive tricalcium phosphate (TCP) (Liu *et al.*, 2008), hydroxyapatite (HA) (Kon *et al.*, 2000), composite of poly(L-lactic acid) and beta-tricalcium phosphate (PLA/TCP) (van der Pol *et al.*, 2010), composite of silicon tricalcium phosphate (Si-TCP) (Mastrogiacomo *et al.*, 2006), composite HA-TCP (Bruder *et al.*, 1998; Arinzeh *et al.*, 2003) and either massive or granular *Porites* coral scaffolds (Petite *et al.*, 2000; Bensaid et *al.*, 2005; Viateau *et al.*, 2007) was established in preclinical, large animal models with long-bone segmental defects. Although studies reporting clinical cases using such constructs for the treatment of either bone-related diseases or large bone defects have been published (Marcacci *et al.*, 1999; Mastrogiacomo *et al.*, 2006; Nair *et al.*, 2010), no prospective and randomized preclinical and clinical studies have yet demonstrated superior effectiveness of such bioengineered bone constructs compared with conventional treatments (i.e. autologous bone grafts). In order to provide clinicians with alternative, effective and novel therapeutic modalities that at least match, and preferably supersede, the clinical efficiency of autologous bone grafts, several aspects, including selection of an appropriate material scaffold need to be determined.

The present study focuses on evaluating the osteogenicity of bone constructs prepared from four clinically available, calcium-based scaffolds combined with autologous MSCs derived from bone marrow. These scaffolds were chosen because they are biocompatible, osteoconductive and support MSC growth and differentiation (Olivier *et al.*, 2004; Chai *et al.*, 2012). Another important characteristic of the scaffolds used in this study is their *in vivo* rate of degradation. Specifically, banked bone is poorly resorbable compared with either β-TCP [$Ca_3(PO_4)_2$] or coral [calcium carbonate ($CaCO_3$) in the form of aragonite] scaffolds. Specifically, corals are more resorbable than β-TCP bioceramics (Guillemin *et al.*, 1987). In the present study, *Porites* and *Acropora*, two different coral scaffolds were used: the former is more resorbable *in vivo* than the latter (Guillemin *et al.*, 1989). The underlying hypothesis of the present study is that osteogenesis mediated by MSCs is affected by the resorption of the substrate material scaffold. In order to investigate the role of the scaffold material in MSC-mediated osteogenesis, and exclude the participation of the scaffolds osteoconductivity in bone formation, assessment of cell-containing construct performance was carried out in an ectopic site in sheep. Under these conditions, osteogenesis resulted from the sole effect of the tissue regeneration function of the transplanted stem cells.

Scaffolds of clinically relevant volume composed of either *Porites* or *Acropora* coral, β-TCP or banked bone were prepared in granular form, seeded with autologous MSCs and assessed *in vivo* in an ectopic sheep model. A major difficulty in conducting a study in an ectopic site was the requirement that each implant (which contained 50–100 individual granules) be held together upon and after implantation to prevent undesirable migration of individual granules into the surrounding tissues. To accomplish this objective, we used the induced membrane technique, which has been used successfully in critical-size segmental bone defects (Viateau *et al.*, 2007; Klaue *et al.*, 2009) and in subcutaneous sites (Catros *et al.*, 2009). For this purpose, pouches were created by implantation of standardized polymethylmethacrylate (PMMA) cylinders into paraspinal subcutaneous sites in sheep. After 6 weeks, these cylinders were removed and each resulting pouch was filled with granules of one of the materials of interest, cell free or seeded with autologous MSCs. Eight weeks after implantation of the constructs, new bone formation and scaffold resorption were determined in explants. New bone formation was compared with the results obtained from the respective cell-free materials implanted. Scaffold resorption was compared with the results obtained from the respective non-implanted cell-free materials.

2. Materials and methods

2.1. *In vitro* studies

2.1.1. Scaffold materials

Four different scaffold materials were tested in the present study. Two of them were coral genera (Biocoral®; Inoteb, La Garenne Colombes, France), and consisted mainly (99%) of calcium carbonate (in the form of aragonite) and (1%) of amino acids. These scaffolds had open, communicating pores had similar configuration (that is, cubes with dimensions $3 \times 3 \times 3$ mm^3 and were *Porites* coral scaffolds (mean pore diameter 250 μm, porosity 49 ± 2%) and *Acropora* coral scaffolds (mean pore diameter 500 μm, porosity 12%). The other two scaffolds were β-TCP (> 95%; Biocetis™; Salon de Provence, France) granules with diameters in the range of 1–3.5 mm (mean pore diameter of 500 ± 100 μm, porosity of 75 ± 10%) and human banked bone consisting of morcelized human corticocancellous bone (Biobank™; Presles en Brie, France) treated using the supercritical CO_2 method (Frayssinet *et al.*, 1998).

X-ray diffractograms, Fourier transform infrared (FT-IR) spectra, and Fourier transform spectrometer Thermo Nicolet, indicated that the granules of β-TCP (Biocetis) were composed of only TCP and mainly comprised of β-TCP (≥ 98 wt%) with traces of α-TCP (≤ 2 wt%). The *Porites* coral, *Acropora* coral and β-TCP were sterilized by autoclaving while the banked bone was sterilized by gamma irradiation according to standard procedures (Viateau *et al.*, 2006).

2.1.2. MSC isolation and culture

Bone marrow (40 ml) was aspirated from the iliac crest of each sheep during the first surgical intervention (that is, at the time of the PMMA cylinder implantation), using

DOI: 10.1002/term

established procedures (Viateau *et al*., 2007). Nucleated cells were counted and suspended in α-minimal essential medium (α-MEM) containing 10% fetal bovine serum (FBS). Primary nucleated cells were seeded at a density of 1×10^5cells/cm^2 of tissue-culture polystyrene surface area. An aliquot of primary cells was used to perform the colony-forming unit efficiency fibroblast assay (CFU-F) as previously described (Fouillard *et al*., 2003). After 3 days of culture, non-adherent cells were discarded during change of supernatant media. The supernatant medium was changed three times a week for the duration of the study. When the cells were confluent (within about 12 days of culture), the MSCs were detached using 0.25% trypsin–ethylenediaminetetraacetic acid (EDTA) and were plated (passage 1) at a density of 3×10^3 cells/cm^2. When 80–90% confluence was reached, the MSCs (passage 1) were detached and cryopreserved in medium containing 90 % FBS and 10% dimethylsulfoxide.

2.1.3. Cell seeding onto scaffolds

Before cell seeding, each scaffold was washed with phosphate-buffered saline (PBS) and immersed in α-MEM containing 10% FBS under standard cell-culture conditions for 24 h. The day before implantation, cryopreserved MSCs were thawed and washed in α-MEM containing 10% FBS. Cell viability was assessed using the Trypan blue exclusion assay. After centrifugation, 2×10^7 MSCs (passage 2) were resuspended in 10 ml of α-MEM containing 10% FBS and seeded on the scaffolds of interest, during this procedure, all scaffolds were contained inside a 50 ml polypropylene tube. To ensure uniform distribution of the MSCs to the scaffolds (static seeding procedure), these tubes were gently rotated by a half-turn every 15 min for 2 h in a humidified 37°C, 5% CO_2/95% air environment. On the day of implantation, the numbers of 'floating' cells in the supernatant medium (i.e. cells that had not adhered to the scaffolds) were counted in the supernatant medium. In order to confirm the distribution/presence of MSCs on the scaffold material, individual granules of each construct prepared from the four types of scaffolds were randomly chosen, the MSCs were labelled using carboxyfluorescein diacetate succinimidyl ester (CFSE) according to standard techniques (Neildez-Nguyen *et al*., 2002) and then examined using fluorescence microscopy.

2.2. *In vivo* studies

2.2.1. Animals

Four, 2-year-old, female Pré-Alpes sheep (each weighing an average of 60 kg) were obtained from a licensed vendor (Institut National de la Recherche Agronomique, Jouy-en-Josas, France) and raised in accordance with the guidelines published by the European Committee for Care and Use of Laboratory Animals (Directive du Conseil 24.11.1986. 86/609/CEE). Animal examinations, housing, feeding and veterinary care were carried out using established procedures described in detail in previous publications by members of our group (Viateau *et al*., 2007). All experiments and procedures involving animals were performed in compliance with regulations of the French Ministry of Agriculture regarding animal experimentation (Act No. 87-847, October 19, 1987, modified May 2001). All animal-related procedures were approved by the Animal Experimentation and Ethic Committee of the Paris-Diderot University (n°9, CEEALV/2009-12-03).

2.2.2. Design of experiments

First, 10–15 sterilized cylinders (height 25 mm; diameter 15 mm) of PMMA were implanted bilaterally into paraspinal subcutaneous sites in each one of four sheep; this procedure induced formation of pouches. Six weeks after PMMA implantation, these cylinders were removed and each resulting pouch was filled with one of the constructs tested. Each animal received constructs from the eight constructs groups. The implants tested were: (1) cell-free *Porites* coral cubes; (2) *Porites* coral cubes loaded with MSCs; (3) cell-free *Acropora* coral cubes; (iv) *Acropora* coral cubes loaded with MSCs; (5) cell-free β-TCP granules; (6) β-TCP granules loaded with MSCs; (7) cell-free banked bone granules; and (8) banked bone granules loaded with MSCs. The volume of each implant tested was equivalent to the volume of the pouches, that is, 4.4 cm^3. The construct-containing pouches were excised 8 weeks post-implantation.

2.2.3. Surgical procedure

Preoperative management of animals. Anaesthesia was induced by intravenous administration of thiopental (12 mg/kg), and was maintained via inhalation of a mixture of oxygen and halothane. Before surgery, all sheep received a prophylactic intramuscular dose (500.000 UI) of penicillin. Each sheep was then positioned in ventral recumbency and the skin (on each side of the dorsal and lumbar spine) was prepared for aseptic surgery and draped using standard sterile procedures.

PMMA implantation. First, 10–15 skin incisions (each 20 mm long) were created bilaterally and perpendicular to the long axis of the sheep spine using a No. 14 Bard Parker blade (Centravet; Maison-Alfort, France). Underlying subcutaneous tissue was undermined with scissors to allow insertion of the PMMA (Sulfix 6®) cylinders (Sulzer; Cham, Swiss). Second, PMMA cylinders (25 mm long and 15 mm in diameter, i.e. equivalent to the volume of the metatarsal bone defect) were implanted into these subcutaneous sites in each of the four sheep. Haemostasis was performed and the incision was closed using a simple intra-dermal continuous suture pattern (and 2 dec Polyglactin 910, Vicryl®) (Johnson & Johnson; Issy-les-Moulineaux, France) followed by skin apposition with simple interrupted sutures (using 2 dec Ethilon®) (Johnson & Johnson;

DOI: 10.1002/term

Table 1. Summary of information pertinent to the constructs implanted into subcutaneous pouches

Construct material	Amount of scaffold material per pouch (g)*	Number of pouches	Number of MSCs per implanted construct*
Acropora	3.31 ± 0.64*	4	N/A
Porites	2.45 ± 0.49	3	N/A
β-TCP	1.64 ± 0.22	3	N/A
Banked bone	0.717 ± 0.18	4	N/A
Acropora + MSCs	4.47 ± 0.79	8	$19 \times 10^6 \pm 3 \times 10^6$
Porites + MSCs	2.53 ± 0.49	8	$16 \times 10^6 \pm 3.5 \times 10^6$
β-TCP + MSCs	1.66 ± 0.33	6	$14 \times 10^6 \pm 2.7 \times 10^6$
Banked bone + MSCs	0.859 ± 0.12	6	$22.7 \times 10^6 \pm 2 \times 10^6$

MSCs, mesenchymal stem cells; β-TCP, beta-tricalcium phosphate.
*Values are mean ± standard deviation.

Issy-les-Moulineaux, France). Special care was taken to ensure that all PMMA cylinders were implanted at similar anatomical locations in the sheep. This procedure induced formation of pouches within 6 weeks after implantation.

Construct implantation. Six weeks after PMMA implantation, these cylinders were palpated through the skin and a 15-mm long transverse skin incision was made perpendicular to the long axis of each cylinder. Underlying subcutaneous tissue was undermined, the membrane was incised perpendicular to the long axis of each cylinder and the PMMA cylinder was removed. The resulting pouch was filled with one of each the constructs of interest. The incision in the membrane was closed using a simple continuous suture pattern (and 2 dec Polyglactin 910, Vicryl). The skin was closed using an intradermal continuous suture pattern (and 2 dec Ethilon). The specific location of the various constructs implanted on the dorsum of each animal was randomly assigned. Details regarding the amount of scaffold material per pouch, the number of pouches, and the number of cells per implanted construct are given in Table 1.

Postoperative management of animals. Postoperative analgesia was provided to all sheep in the form of intravenous injections of: (1) tramadol as Contramal® (2 ml IV) (Grünenthal SAS, Levallois-Perret, France) and flunixin meglumin as Finadyne® (2 mg/kg) (Grünenthal SAS, Levallois-Perret, France) which were administered 30 min before the end of each surgical procedure; and (2) meloxicam as Metacam® (0.5 mg/kg) (Boehringer Ingeheim, Reims, France), which was administered 72 h after completion of the surgical procedure. Skin wounds were treated locally using an antiseptic solution (Orospay®) (Centravet; Maison-Alfort, France); no bandages were applied. Postoperatively, the animals were monitored daily for wound-related complications and treated as and when needed.

Specimen explantation. Eight weeks after implantation, a 15-mm long transverse skin incision was made perpendicular to the long axis of each implant-containing pouch, which were thereafter explanted. Haemostasis was performed and the incision was closed. Each explanted pouch (containing implants) was fixed in neutral 10% formalin buffer and used for radiographic and histology analysis.

Non-implanted control. Non-implanted control pouches were also prepared cell-free for each scaffold material tested, using latex pouches filled with the same amount of scaffold material as described in Section 2.2.2. (Design of experiments). These non-implanted control pouches contained scaffolds of the same volume as those placed in the implanted pouches. The contents of the non-implanted control pouches were used to evaluate resorption of the scaffold materials tested.

2.2.4. Analysis of explants

The radiopacity of the construct-containing pouches was assessed using X-ray radiography (Faxitron™) (Edimex; Le Plessis Grammoire, France). The values of digital radiography pixels were proportional to specimen radiopacity and were expressed as 'grey' levels; in an 8-bit image, a grey level had a value from 0 to 255. IMAGE J software (NIH) (Nikon France; Champigny-sur-Marne, France) was used to determine the mean grey level of the construct-containing pouches retrieved and of their respective non-implanted control pouches. A region of interest [using a 1-cm diameter region of interest (ROI) located in the centre of each specimen] was chosen on each radiograph and the respective mean grey level was quantified.

The radiopacity volume of the constructs contained in each pouch was determined using micro-X-ray computed tomography (μCT). All samples were scanned using a desktop Micro-CT (Skyscan 1172; Skyscan, Aartselaar, Belgium), with 80 KV source voltage, 100 μA source current and 26.6 μm image pixel size. Each sample was rotated 180° (using a rotation step of 0.5°); the exposure time was 0.4 s. NRECON (v.1.6.6, Skyscan) and CT-ANALYZER (v.1.12, Skyscan) were used for three dimensional reconstruction and analysis.

The explanted construct-containing pouches were then processed for histology using standard techniques as previously described (Petite *et al*., 2000). Briefly, the samples were dehydrated (in graded series of increasing alcohol concentration) and then embedded in PMMA resin. The PMMA-embedded blocks were cut using a circular, water-cooled, diamond saw (Leitz 1600; Leica, Nussloch, Germany) (200−300 μm). Sections from the proximal, median and distal transverse planes of each specimen were selected. Each section was ground to a thickness of 100 μm, polished and the surface-stained using Stevenel blue and van Gieson picro-fuchsin, according to standard procedures (Petite *et al*., 2000). All stained sections were examined using light microscopy (Leica).

Histomorphometry was carried out using a microscope linked to an image processing system (NIS Element; Nikon, France) through a 3-CCD video camera (DXC-930P; Nikon) (Nikon France; Champigny-sur-Marne, France). All scaffold and bone images (whole-section samples) were pseudocoloured in black and red, respectively, using NIS ELEMENT software (Nikon France; Champigny-sur-Marne, France). The areas of newly-formed bone were measured. All histomorphometric and microscopic analyses were performed under blinded conditions.

2.3. Statistical analysis

Numerical data were analysed using *t*-test analysis to assess statistical significance. The confidence interval was set at 95%, and the significance level at $p < 0.05$ for the histomorphometric and X-ray analyses.

3. Results

3.1. *In vitro* studies

The sheep bone marrow aspirates contained 12–48 $\times$ 10^6 mononuclear cells/ml. The mean number of CFU-F in the bone marrow aspirates of the four sheep tested, was 75.25 $\pm$ 24.75 per 10^6 mononuclear cells. The number of MSCs that did not adhere on the scaffolds was less than 10% of the total seeded cells. Cell staining with CFSE revealed the presence of adherent cells onto the tested scaffolds.

3.2. *In vivo* studies

The surgical procedures used were well tolerated by all animals, which recovered uneventfully from surgery-related anaesthesia. At the time of specimen retrieval (i.e. 8 weeks after implantation), all implants were contained within their respective pouches. Three pouches were not used because of dehiscence of the skin suture line overlying the PMMA cylinders. A total of 42 pouches that had been filled with implants were available for the analyses. These are described in the sections that follow.

3.3. Scaffold material resorption

Owing to their radiopacity, the four scaffold materials used in the present study were easily visualized by X-rays.

Eight weeks after implantation, the explanted pouches containing either cell-free *Acropora* coral scaffolds or cell-free *Porites* coral scaffolds showed lower radiopacity than their respective non-implanted, control pouches (Figure 1a). This observation provided evidence of an ongoing process of resorption/biodegradation of the coral scaffolds tested. In contrast, the explanted pouches containing either β-TCP or banked bone specimens exhibited similar radiopacity to their respective non-implanted, control pouches (Figure 1a). There was no radiographic evidence of resorption of either the β-TCP or banked bone after 2 months of ectopic implantation. Quantitative analyses of two-dimensional, digital radiograms and of three-dimensional μCT were performed. The mean grey level of pouches retrieved after 8 weeks of implantation containing either cell-free *Acropora* coral scaffolds (206.8 $\pm$ 10.5, $n = 4$), or *Acropora* coral constructs containing MSCs (222 $\pm$ 10.7, $n = 8$), or cell-free *Porites* coral scaffolds (185.1 $\pm$ 12.2, $n = 3$) or *Porites* coral constructs containing MSCs (177 $\pm$ 11, $n = 8$) exhibited a significant ($p < 0.001$) decrease in the mean grey level compared with the results obtained from the non-implanted control pouches (cell-free) containing either *Acropora* coral scaffolds (252 $\pm$ 2.3, $n = 8$) or *Porites* coral scaffolds (250 $\pm$ 3.6, $n = 8$) (Figure 1b). Comparison of the mean grey levels of pouches containing either *Porites* or *Acropora* coral constructs 8 weeks after implantation revealed that the *Porites* coral scaffolds were more resorbed ($p < 0.001$) than the *Acropora* coral scaffolds (Figure 1b,c).

In contrast, pouches filled with either cell-free β-TCP scaffolds ($n = 3$), or β-TCP constructs containing MSCs ($n = 6$), cell-free banked bone scaffolds ($n = 4$) or banked bone constructs containing MSCs ($n = 4$) retrieved after 8 weeks of implantation had mean grey levels similar to their respective, non-implanted, controls pouches. These values were, respectively: 243.2 $\pm$ 6.6 vs. 247.8 $\pm$ 6, 240.7 $\pm$ 4.9 vs. 247.8 $\pm$ 6, 211.5 $\pm$ 11.2 vs. 211.5 $\pm$ 11.1 and 223.3 $\pm$ 14.8 vs. 211.5 $\pm$ 11.1 (Figure 1b).

We also evaluated the radiopacity volume of the constructs obtained from pouches retrieved after 8 weeks of implantation using μCT. The radiopacity volume of the non-implanted pouches and of the cell-free scaffold constructs containing pouches retrieved 8 weeks after implantation corresponded to the scaffold volume. The radiopacity volume of scaffold constructs containing MSCs corresponded to the scaffold and new bone formation volume. The radiopacity volume of pouches filled with either cell-free *Acropora* coral (24.39 $\pm$ 9.48 mm^3), *Acropora*

DOI: 10.1002/term

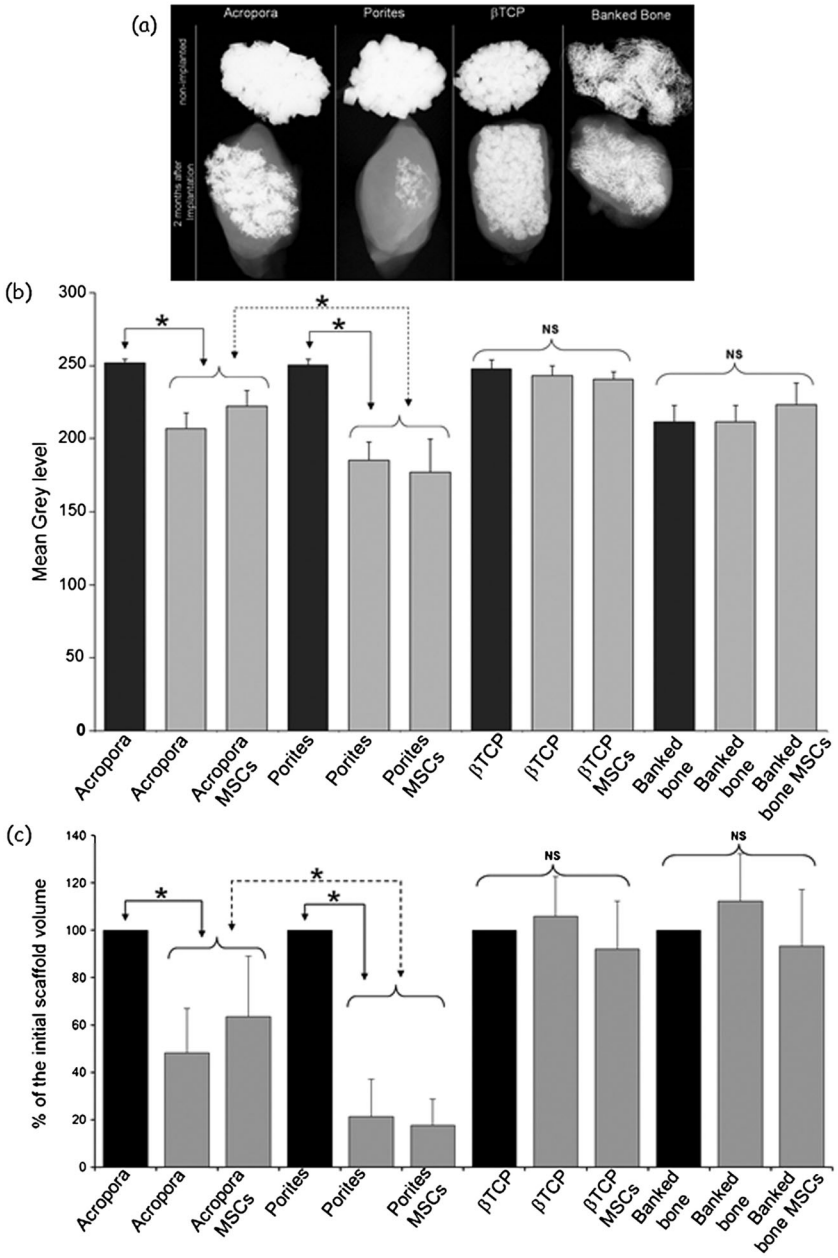

Figure 1. (a) Representative X-ray radiogram of pouches filled (sequentially from left to right) with cell-free *Acropora* coral, cell-free *Porites* coral, cell-free beta-tricalcium phosphate (β-TCP) and cell-free banked bone, either non-implanted or retrieved 2 months after implantation are shown on the top and bottom rows, respectively. (b) Comparison of the radio-opacity of pouches containing one of the eight different biomaterials tested. (c) Comparison of the degree of scaffold material resorption of the eight different constructs when they were maintained in the pouches tested for 8 weeks after implantation. Filled bars represent non-implanted pouches containing the respective biomaterials. Tinted bars represent pouches containing the respective biomaterials 8 weeks after implantation. Values are mean ± standard deviation. MSCs, mesenchymal stem cells

coral containing MSCs (32.07 ± 13.93 mm^3), cell-free *Porites* coral scaffolds (16.81 ± 12.33 mm^3), *Porites* coral containing MSCs (13.92 ± 8.7 mm^3), cell-free β-TCP scaffolds (20.20 ± 4.39 mm^3), β-TCP constructs containing MSCs (21.93 ± 4.15 mm^3), cell-free banked bone scaffolds (8.45 ± 1.34 mm^3) and banked bone containing MSCs (7.09 ± 1.82 mm^3), retrieved after 8 weeks of implantation were compared with the results obtained from non-implanted control pouches (cell-free) (100% of scaffold volume) filled with either *Acropora* coral scaffolds (50.49 ± 9.53 mm^3), *Porites* coral scaffolds (78.44 ± 11.71 mm^3), β-TCP scaffolds (23.21 ± 3.68 mm^3) or banked bone scaffolds (7.60 ± 1.82 mm^3). The radiopacity volume of pouches containing cell-free scaffolds and scaffold constructs containing MSCs after 8 weeks of implantation was similar. We compared the percentage of the remaining scaffold volume for each group of implanted pouches with their respective non-implanted control pouches. To determine the degree of scaffold resorption after 8 weeks of implantation, the volume of the remaining scaffold was expressed as percentage of the initial scaffold volume (non-implanted pouch) (Figure 1c). Comparison of the degree of scaffold resorption between pouches containing either *Porites*

DOI: 10.1002/term

or *Acropora* coral constructs 8 weeks after implantation revealed that the *Porites* coral scaffolds were resorbed more ($p < 0.001$) than the *Acropora* coral scaffolds (Figure 1c). In contrast, pouches containing either β-TCP or banked bone constructs 8 weeks after implantation had a scaffold volume similar to their respective non-implanted control pouches.

These results confirmed that coral (i.e. both *Acropora* and *Porites*) scaffold resorption was more extensive than that observed with either the β-TCP or banked bone specimens tested (Figure 1c).

3.4. New bone formation

At 2 months post-implantation, a vascularized fibrous tissue surrounded all granule scaffolds and invaded the pores of the scaffolds of all implants tested without MSCs (Figure 2a–e). There was no sign of inflammation except in the case of one pouch containing cell-free banked bone (Figure 2f). In pouches containing cell-free *Acropora* coral or *Porites* coral, β-TCP or banked bone scaffolds there was no bone or cartilage formation (Figure 2).

In contrast, constructs containing MSCs exhibited systematically – albeit to different extents – woven bone with active osteoblasts (Figure 3a–d). In these constructs, bone lined by osteoblasts was closely apposed to the scaffold material surfaces. In the case of either the *Porites* coral or *Acropora* coral loaded with MSCs (Figure 3a,b) woven bone was observed both on the coral surface and in the surrounding fibrous tissue formed. In both cases, the woven bone appeared normal, was aligned, contained osteocytes in lacunae and was coated with osteoblasts. Bone formation occurred through bone apposition and mesenchymal cell condensation (Figure 3e). In all constructs tested no cartilage was formed.

Analysis of the histomorphometric images provided evidence that the surface area of the newly formed bone was significantly ($p < 0.05$) greater in the coral constructs than in either the β-TCP or the banked bone one (Figure 4).

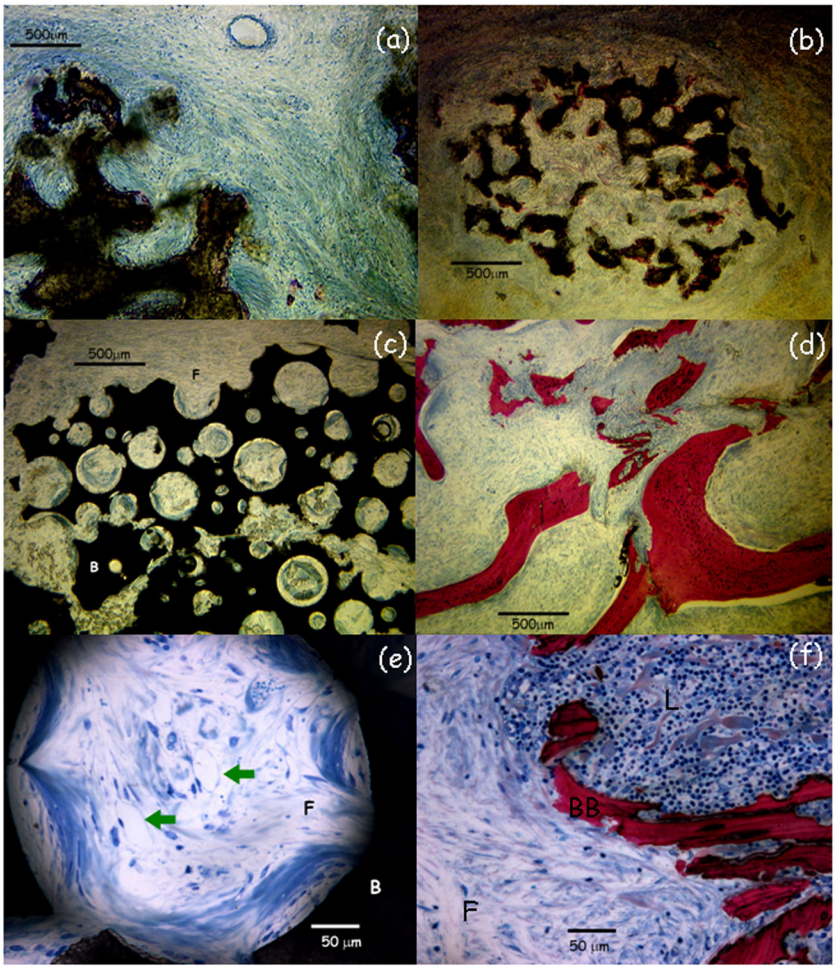

Figure 2. Representative histology results of undecalcified pouches containing cell-free scaffolds retrieved 8 weeks after subcutaneous ectopic implantation in sheep. Each pouch contained one of the following biomaterials: (a) *Acropora* coral; (b) *Porites* coral; (c) beta-tricalcium phosphate (β-TCP); and (d) banked bone. Stains: Stevenel Blue and van Gieson picro-fuchsin. Cells and fibrous tissue (F) stained blue, β-TCP stained black (B) and Banked bone stained red (BB). Scale bar = 500 µm. (e) Enlargement of (c) illustrates the presence of fibrous tissue (F) stained blue and the presence of capillaries (green arrows) within the pores of the β-TCP scaffold. Scale bar = 50 µm. (f) Enlargement of (d) illustrating the presence of a lymphoid cluster (L) observed only in one pouch containing cell-free banked bone. Scale bar = 50 µm

DOI: 10.1002/term

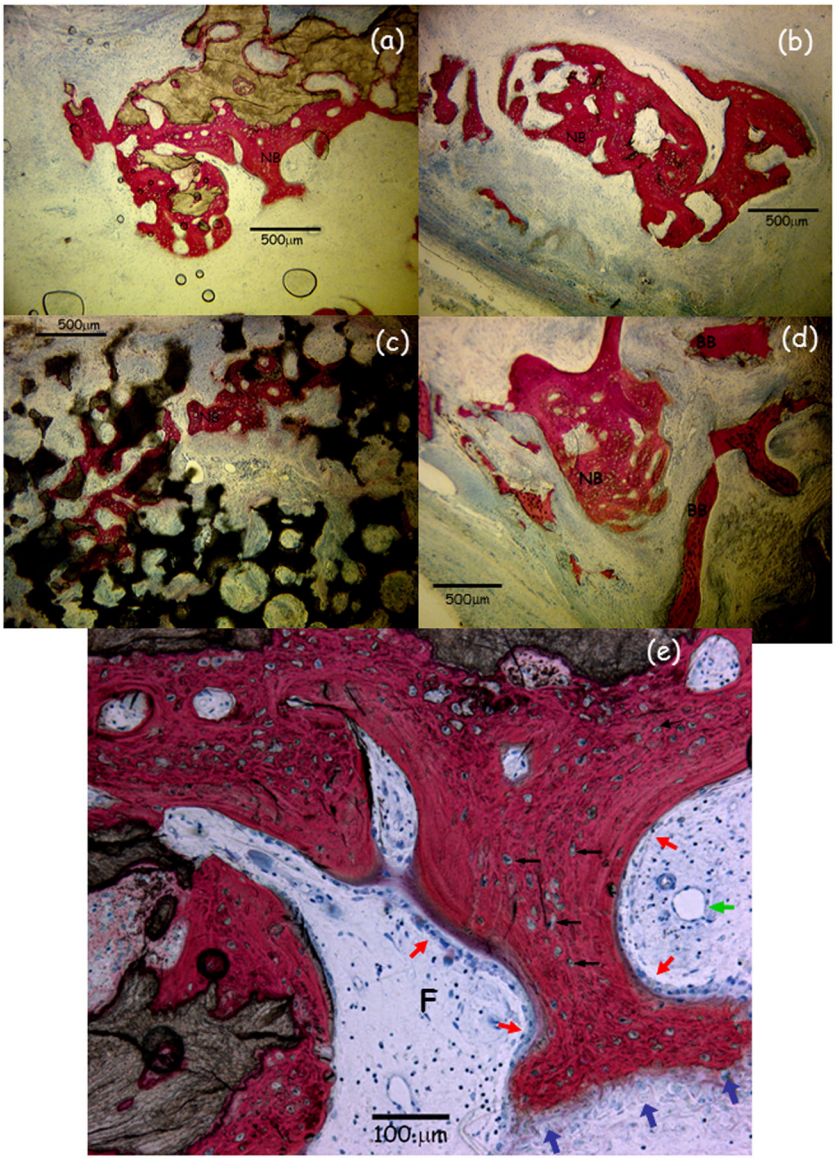

Figure 3. Representative histology results of pouches with mesenchymal stem cell (MSC)-containing constructs retrieved 8 weeks after subcutaneous ectopic implantation in sheep. Each pouch contained one of the following materials: (a) *Acropora* coral containing MSCs; (b) *Porites* coral containing MSCs; (c) beta-tricalcium phosphate (β-TCP) containing MSCs; and (d) banked bone containing MSCs. Stains: Stevenel Blue and von Gieson picro-fuchsin. New bone (NB) stained red, banked bone stained red, while cells and fibrous tissue stained blue; *Acropora*, *Porites* and β-TCP stained brown/black. Scale bar = 500 µm. (e) Enlargement of frame (a). In this case, cells and fibrous tissue stained blue, *Acropora* coral stained brown and woven bone stained red. New bone containing osteoblasts and osteocytes was present on the surface of the *Acropora* scaffold material and stained red. The new bone was normal and aligned with the osteoblast layer. In (e) the black arrows point to osteocytes in lacunae, the red arrows point to areas of bone apposition, the blue arrows point to areas of mesenchymal cell condensation and the green arrows point to capillaries. Stains: Stevenel Blue and von Gieson picro-fuchsin. Scale bar = 100 µm

4. Discussion

Banked bone, TCP and coral are osteoconductive materials that have been used clinically as delivery vehicles for MSCs to obtain bone repair in several animal models (Kon *et al.*, 2000; Petite *et al.*, 2000; Bensaid *et al.*, 2005; Viateau *et al.*, 2006, 2007, 2010; Cancedda *et al.*, 2007; Kruyt *et al.*, 2007). Comparison of the performance of the aforementioned materials as scaffolds for the delivery of osteocompetent cells is, however, difficult to determine because of differences pertaining to (1) the methods of preparation of the constructs, (2) the anatomical location in which constructs were implanted, (3) the species involved and (4) the criteria used to evaluate the osteogenic ability of the constructs tested. Such lack of comparative information precludes a rational choice of scaffolds for clinical studies. In an attempt to fill this knowledge gap, the respective osteogenic ability of clinically relevant size bone constructs prepared from the aforementioned scaffold materials and containing MSCs, was therefore compared. To this end, tissue constructs of clinically relevant volume were implanted in an ectopic sheep model and their osteogenic ability assessed. The

DOI: 10.1002/term

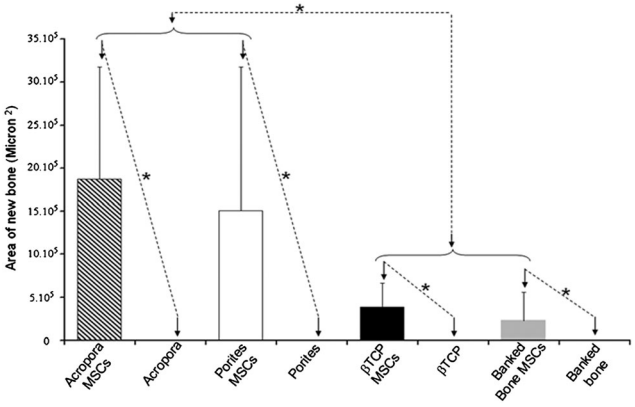

Figure 4. Areas of new bone formation in pouches filled with either mesenchymal stem cell (MSC)-containing *Acropora* coral constructs (hatched bar), cell-free *Acropora* coral scaffolds, MSC-containing *Porites* coral constructs (white bar), cell-free *Porites* coral scaffolds, MSC-containing beta-tricalcium phosphate (β-TCP constructs (filled bar), cell-free β-TCP scaffolds, MSC-containing banked bone constructs (tinted bar), and cell-free banked bone scaffolds retrieved after 8 weeks of implantation. Significantly (*$p < 0.05$) more new bone was present when the scaffolds tested were seeded with MSCs. The area of new bone was significantly ($p < 0.05$) greater in the MSC-containing coral constructs than in either the MSC-containing β-TCP or MSC-containing banked bone constructs. Values are mean ± standard deviation**

ectopic model was chosen to specifically assess the influence of MSCs *per se* on bone formation, excluding the influence of osteoconduction on the process of new bone formation.

In the present study, the scaffolds tested were implanted in cavities delineated by a previous PMMA-induced membrane (Masquelet *et al*., 2000; Viateau *et al*., 2006). Previous studies performed with rabbits and sheep reported that such membrane induced in subcutaneous sites had no osteogenic potential (Catros *et al*., 2009; Viateau *et al*., 2010). The results of the present study showed that all cell-free scaffolds tested did not exhibit osteogenicity properties (Figures 2 and 4) confirming that the subcutaneous pouch model provided a 'neutral' microenvironment in which osteocompetent cells were required in order to obtain new bone formation.

The results presented in this study that the *Porites* coral scaffolds had a higher rate of resorption than the *Acropora* scaffolds are in agreement with results reported in previous studies that used an orthotopic model (Guillemin *et al*., 1989). These coral materials had similar chemical composition ($CaCo_3$) but differ in porosity volume ($V_{Porites}$ = 49 ± 2% vs. $V_{Acropora}$ = 12 ± 4%) and mean pore diameter ($\varnothing_{Porites}$ = 250 μm vs. $\varnothing_{Acropora}$ = 500 μm): consequently, the *Porites* scaffolds had larger surface area. A possible explanation for the higher rate of resorption of the *Porites* scaffolds observed in the present study is, therefore, the result of their larger surface area, which favoured increased interactions with the physicochemical factors responsible for resorption of that scaffold material (Guillemin *et al*., 1987).

The absence of osteoinductivity observed with the β-TCP scaffolds used in the present study contrasted with previous studies in which cell-free TCP implanted in either an ectopic or an intramuscular site promoted new bone formation (Yuan *et al*., 2001). This difference may be result from biological factors or from microenvironmental aspects specific to the 'pouch model' as well as from material aspects, including the chemistry, geometry and porous structure of the TCP scaffolds that may affect their osteoinductivity (Yuan *et al*., 2010). In addition, β-TCP scaffolds (with or without MSCs) did not exhibit significant resorption during the time period of the present study. Usually TCP is removed rapidly by a combination of resorption and/or dissolution processes (Kitamura *et al*., 2004; Arinzeh *et al*., 2005; Kamitakahara *et al*., 2008). A possible explanation for this difference is that the closed environment of the pouch led to rapid local saturation of calcium and phosphate ions, preventing further dissolution of the enclosed scaffolds. Further investigations are needed to elucidate the protective effect of the pouch model on TCP resorption/dissolution.

Upon implantation, banked bone usually exhibits immunogenicity owing to major histocompatibility complex (MHC) proteins which are present on the bone-marrow cell membranes (Friedlaender, 1991). To reduce this antigenicity, the banked bone used in the present study was treated with supercritical CO_2, a powerful solvent used in extracting lipids from bone. Upon implantation, the banked bone pretreated using this method integrated well in sheep bone defects, in contrast to untreated allograft bone which resorbed extensively (Frayssinet *et al*., 1998). In this respect, the present study confirmed the efficacy of supercritical CO_2 treatment in preventing inflammation and resorption of allograft bone after implantation. The results of the present study, however, are in sharp contrast to those of another published study which reported extensive resorption of allograft bone, either cell-free or loaded with autologous MSCs, implanted intramuscularly in goats (Eniwumide *et al*., 2007). This disagreement may result from differences in the respective animal models but, in the authors' opinion, most likely reflects differences in the efficacy of the process used to clean allograft bone before implantation. A tempting explanation for the massive resorption of implanted allografts observed in the study by Eniwumide *et al*. (2007) is that the process (i.e. a 20-min immersion in chloroform–methanol) used to extract lipid from the allograft bone did not remove all bone marrow elements from specimens. Further investigations are needed to definitively resolve this issue. Alternatively, it is possible that the induced membrane created an environment that limited scaffold resorption in the present study. Indeed, Masquelet *et al*. (2000) proposed that one of the advantages of the induced membrane model is that it prevents graft resorption during the early post-implantation stages. There are, however, two major limitations when using the subcutaneous pouch: (1) the model is cumbersome because it requires an extra surgical operation to form a pseudomembrane, and (2) the ectopic location is

DOI: 10.1002/term

susceptible to mechanical shear stresses and to effects from surrounding various tissues (such the underlying muscle and overlying skin). In the present study, new bone was formed on banked bone only when it had been seeded with MSCs (compare Figure 2d and Figure 3d); although not consistently, this bone co-localized several times with areas of banked bone resorption.

In the present study, new bone formation was observed within all types of constructs seeded with MSCs and tested; these results provided evidence that the MSCs rendered the scaffold osteogenic (Figures 3 and 4). This study tested the hypothesis that, in the presence of MSCs, the rate of scaffold resorption influenced the process of new bone formation. Evidence supporting this hypothesis was provided by the results that both β-TCP and allograft bone (the two least-resorbable among the materials tested) (Figure 1), showed the smallest amount of new bone formation (Figure 4). Lack of degradation of the substrate material in the MSC-containing-constructs and the concurrent reduced rate of new bone formation is in agreement with literature reports that resorption of silicon-stabilized TCP ceramics is needed for new bone formation to occur and that there is coupling between bone formation and scaffold resorption (Mastrogiacomo *et al*., 2007; Papadimitropoulos *et al*., 2007). The results of the present study are not only in agreement with these literature reports but also extend the scope of the field to tissue constructs of clinically relevant bone size. In addition, the results of the present study identified coral as the best scaffold material to support the osteogenic potential of MSCs under the conditions tested. Although the pouch model provides a relatively inexpensive evaluation and comparison of the osteogenicity of tissue constructs, it does not take into account the osteoconductive properties of the cell-free material substrate. For this reason, and in order to evaluate the efficacy of tissue constructs for bone repair, the more promising constructs identified in the present study must be further examined and validated in the intra-osseous set-up in relevant, large animal models under load-bearing conditions.

5. Conclusions

This is the first report describing successful use of an ectopic sheep model to investigate, and to compare, implanted material resorption and new bone formation of various clinically relevant biomaterial scaffolds. The present study demonstrated that, in the absence of MSCs, no bone formation occurred. However, in the presence of MSCs there was positive correlation between scaffold material resorption and new bone formation. In the present study, coral scaffolds containing MSCs supported the best new bone formation.

Acknowledgements

The authors thank Dr N. Guillemin (for her kind assistance with this study), Prof. R. Bizios (for her valuable comments on the manuscript), Biocoral, Inc., (for donating the coral scaffolds), Biobank, Inc., (for donating the banked bone) and Valentin Myrtil (for excellent technical support). We also acknowledge financial support from la Delegation à la Recherche Clinique de l'Assistance Publique des Hôpitaux de Paris, from Centre National de Recherche Scientifique, and from ANR therabone.

Conflict of interest

The authors declare that they have no competing financial interests.

References

Arinzeh TL, Peter SJ, Archambault MP, *et al*. 2003; Allogeneic mesenchymal stem cells regenerate bone in a critical-sized canine segmental defect. *J Bone Joint Surg Am* **85A**: 1927–1935.

Arinzeh TL, Tran T, Mcalary J, *et al*. 2005; A comparative study of biphasic calcium phosphate ceramics for human mesenchymal stem-cell-induced bone formation. *Biomaterials* **26**: 3631–3638.

Bensaid W, Oudina K, Viateau V, *et al*. 2005; De novo reconstruction of functional bone by tissue engineering in the metatarsal sheep model. *Tissue Eng* **11**: 814–824.

Bianco P, Robey PG. 2001; Stem cells in tissue engineering. *Nature* **414**: 118–121.

de Boer HH, Wood MB. 1989; Bone changes in the vascularised fibular graft. *Acta Biomater* **71**: 374–378.

Bruder SP, Kraus KH, Goldberg VM, *et al*. 1998; The effect of implants loaded with autologous mesenchymal stem cells on the healing of canine segmental bone defects. *J Bone Joint Surg Am* **80**: 985–996.

Cancedda R, Bianchi G, Derubeis A, *et al*. 2003; Cell therapy for bone disease: a review of current status. *Stem Cells* **21**: 610–619.

Cancedda R, Giannoni P, Mastrogiacomo M. 2007; A tissue engineering approach to bone repair in large animal models and in clinical practice. *Biomaterials* **28**: 4240–4250.

Caplan AI. 2005; Mesenchymal stem cells: cell based reconstructive therapy in orthopedics. *Tissue Eng* **11**: 1198–1211.

Catros S, Zwetyenga N, Bareille R, *et al*. 2009; Subcutaneous-induced membranes have no osteoinductive effect on macroporous HA-TCP in vivo. *J Orthop Res* **27**: 155–161.

Chai YC, Carlier A, Bolander J, *et al*. 2012; Current views on calcium phosphate osteogenicity and the translation into effective bone regeneration strategies. *Acta Biomater* **8**: 3876–3887.

Eniwumide JO, Yuan H, Cartmell SH, *et al*. 2007; Ectopic bone formation in bone marrow stem cell seeded calcium phosphate scaffolds as compared to autograft and (cell seeded) allograft. *Eur Cell Mater* **14**: 30–38.

Fouillard L, Bensidhoum M, Bories D, *et al*. 2003; Engraftment of allogeneic mesenchymal stem cells in the bone marrow of a patient with severe idiopathic aplastic anemia improves stroma. *Leukemia* **17**: 474–476.

Frayssinet P, Rouquet N, Mathon D, *et al*. 1998; Histological integration of allogeneic cancellous bone tissue treated by supercritical CO2 implanted in sheep bones. *Biomaterials* **19**: 2247–2253.

Friedenstein AJ, Piatetzky-Shapiro II, Petrakova KV. 1966; Osteogenesis in transplants of bone marrow cells. *J Embryol Exp Morphol* **16**: 381–390.

Friedenstein AJ, Petrakova KV, Kurolesova AI, *et al*. 1968; Heterotopic of bone marrow. Analysis of precursor cells for osteogenic and hematopoietic tissues. *Acta Biomater* **6**: 230–247.

Friedlaender GE. 1991; Bone allografts: the biological consequences of immunological events. *J Bone Joint Surg Am* **73**: 1119–1122.

Guillemin G, Patat JL, Fournie J, *et al*. 1987; The use of coral as a bone graft substitute. *J Biomed Mater Res* **21**: 557.

Guillemin G, Meunier A, Dallant P, *et al*. 1989; Comparison of coral resorption and bone apposition with two natural corals of different porosities. *J Biomed Mater Res* **23**: 765–779.

Han CS, Wood MB, Bishop AT, *et al*. 1992; Vascularized bone transfer. *J Bone Joint Surg Am* **74**: 1441.

Kamitakahara M, Ohtsuki C, Miyazaki, T. 2008; Review paper: behavior of ceramic biomaterials derived from tricalcium phosphate in physiological condition. *J Biomater Appl* **23**: 197–212.

Kitamura M, Ohtsuki C, Iwasaki H, *et al*. 2004; The controlled resorption of porous alpha-tricalcium phosphate using a hydroxypropylcellulose coating. *J Mater Sci Mater Med* **15**: 1153–1158.

Klaue K, Knothe U, Anton C, *et al*. 2009; Bone regeneration in long-bone defects: tissue compartmentalisation? *In vivo* study on bone defects in sheep. *Injury* **40** (Suppl 4): S95–S102.

Kon E, Muraglia A, Corsi A, *et al*. 2000; Autologous bone marrow stromal cells loaded onto porous hydroxyapatite ceramic accelerate bone repair in critical-size defects of sheep long bones. *J Biomed Mater Res* **49**: 328–337.

Kruyt MC, Dhert WJ, Oner FC, *et al*. 2007; Analysis of ectopic and orthotopic bone formation in cell-based tissue-engineered constructs in goats. *Biomaterials* **28**: 1798–1805.

Liu G, Zhao L, Zhang W, *et al*. 2008; Repair of goat tibial defects with bone marrow stromal cells and beta-tricalcium phosphate. *J Mater Sci Mater Med* **19**: 2367.

Logeart-Avramoglou D, Anagnostou F, Bizios R, *et al*. 2005; Engineering bone: challenges and obstacles. *J Cell Mol Med* **9**: 72–84.

Liu G, Zhao L, Zhang W, *et al*. 2008; Repair of goat tibial defects with bone marrow stromal cells and beta-tricalcium phosphate. *J Mater Sci Mater Med* **19**: 2367–2376.

Marcacci M, Kon E, Zaffagnini S, *et al*. 1999; Reconstruction of extensive long-bone defects in sheep using porous hydroxyapatite sponges. *Calcif Tissue Int* **64**: 83–90.

Masquelet AC, Fitoussi F, Begue T, *et al*. 2000; Reconstruction of the long bones by the induced membrane and spongy autograft. *Ann Chir Plast Esthet* **45**: 346–353.

Mastrogiacomo M, Corsi A, Francioso E, *et al*. 2006; Reconstruction of extensive long bone defects in sheep using resorbable bioceramics based on silicon stabilized tricalcium phosphate. *Tissue Eng* **12**: 1261–1273.

Mastrogiacomo M, Papadimitropoulos A, Cedola A, *et al*. 2007; Engineering of bone using bone marrow stromal cells and a silicon-stabilized tricalcium phosphate bioceramic: evidence for a coupling-between bone formation and scaffold resorption. *Biomaterials* **28**: 1376–1384.

May JW, Jupiter JB, Weiland AJ, *et al*. 1989; Clinical classification of post-traumatic tibial osteomyelitis. *J Bone Joint Surg Am* **71**: 1422–1428.

Nair MB, Varma H, Shenoy SJ, *et al*. 2010; Treatment of goat femur segmental defects with silica-coated hydroxyapatite-one-year follow-up. *Tissue Eng Part A* **16**: 385–391.

Neildez-Nguyen TM, Wajcman H, Marden MC, *et al*. 2002; Human erythroid cells produced *ex vivo* at large scale differentiate into red blood cells in vivo. *Nat Biotechnol* **20**: 467–472.

Olivier V, Faucheux N, Hardouin, P. 2004; Biomaterial challenges and approaches to stem cell use in bone reconstructive surgery. *Drug Discov Today* **9**: 803–811.

Papadimitropoulos A, Mastrogiacomo M, Peyrin F, *et al*. 2007; Kinetics of *in vivo* bone deposition by bone marrow stromal cells within a resorbable porous calcium phosphate scaffold: an X-ray computed microtomography study. *Biotechnol Bioeng* **98**: 271–281.

Petite H, Viateau V, Bensaid W, *et al*. 2000; Tissue-engineered bone regeneration. *Nat Biotechnol* **18**: 959–963.

van der Pol U, Mathieu L, Zeiter S, *et al*. 2010; Augmentation of bone defect healing using a new biocomposite scaffold: an *in vivo* study in sheep. *Acta Biomater* **6**: 3755–3762.

Viateau V, Guillemin G, Calando Y, *et al*. 2006; Induction of a barrier membrane to facilitate reconstruction of massive segmental diaphyseal bone defects: an ovine model. *Vet Surg* **35**: 445–452.

Viateau V, Guillemin G, Bousson V, *et al*. 2007; Long-bone critical-size defects treated with tissue-engineered grafts: a study on sheep. *J Orthop Res* **25**: 741–749.

Viateau V, Bensidhoum M, Guillemin G, *et al*. 2010; Use of the induced membrane technique for bone tissue engineering purposes: animal studies. *Orthop Clin North Am* **41**: 49–56.

Yuan H, De Bruijn JD, Li Y, *et al*. 2001; Bone formation induced by calcium phosphate ceramics in soft tissue of dogs: a comparative study between porous alpha-TCP and beta-TCP. *J Mater Sci Mater Med* **12**: 7–13.

Yuan H, Fernandes H, Habibovic P, *et al*. 2010; Osteoinductive ceramics as a synthetic alternative to autologous bone grafting. *Proc Natl Acad Sci USA* **107**: 13614–13619.